Stony Brook University

Quantification of the *peroneus longus* groove in primate cuboids: Implications for *Ardipithecus ramidus*

A Thesis Presented

by

Erin Jean Achilles

to

The Graduate School

in Partial Fulfillment of the

Requirements

for the Degree of

Master of Arts

in

Anthropology

(Physical Anthropology)

Stony Brook University

August 2012

Stony Brook University

The Graduate School

Erin Jean Achilles

We, the thesis committee for the above candidate for the

Master of Arts degree, hereby recommend

acceptance of this thesis.

Frederick E. Grine
Professor, Department of Anthropology

Karen L. Baab
Assistant Professor, Department of Anthropology

Biren Patel
Research Instructor, Department of Anatomical Sciences

Caley M. Orr
Research Instructor, Department of Anatomical Sciences

This thesis is accepted by the Graduate School

Charles Taber

Interim Dean of the Graduate School

Abstract of the Thesis

Quantification of the *peroneus longus* groove in primate cuboids: Implications for *Ardipithecus ramidus*

by

Erin Jean Achilles

Master of Arts

in

Anthropology

(Physical Anthropology)

Stony Brook University

2012

Significant debate surrounds the question of locomotor pattern in the last common ancestor (LCA) of chimpanzees and humans. Traditionally, most researchers have agreed that the morphology of the LCA was similar to that of extant African apes. However, recent analyses of the foot of the possible stem hominin *Ardipithecus ramidus* by Lovejoy et al. (2009) suggest the earliest hominins may have possessed a locomotor pattern more similar to that of a monkey. This argument is based in part on the morphology of the groove for the *peroneus longus* tendon located on the cuboid bone. The orientation of this groove is thought to relate to locomotor pattern, and a qualitative assessment of this angle in *A.ramidus* suggests that it compares favorably with the Old World monkey condition. However, no quantification of the groove angle is provided. In this study, I quantified the angle of the groove for *peroneus longus* relative to the facet for the fourth metatarsal using eight landmarks on the cuboid, analyzing both landmark

data and linear and angular measurements derived from this data. A comparative sample including extant humans, apes, and monkeys, as well as fossil hominins and apes, shows that groove angle can be used to distinguish some taxonomic groups, but is highly variable within taxa. Additionally, there is only a weak link between particular locomotor patterns and groove angle. Therefore, this metric should not be used to make assumptions about locomotor behavior in *A.ramidus* or other fossil species and is not relevant to reconstructions of locomotor pattern in the human-chimpanzee LCA.

Table of Contents

List of Figures

List of Tables

Acknowledgments

Above all, I would like to thank Biren Patel and Caley Orr, without whom this project would not have been possible. Biren: thank you for giving me the idea for this project and for helping me to see it through over the course of the last year. Caley: thank you for being so supportive of this project, from answering my questions to writing the matlab code. And to both of you, thank you for supporting my decision to use this as my human evolution project, then as a qualifier, then as a Master's thesis, and for dealing with all of my indecision in between!

I would also like to thank Karen Baab for providing me with useful instruction on methods, from teaching me how to use the MicroScribe to running a PCA to figuring out what statistics to use. I appreciate your patience and your ability to explain confusing concepts in a completely understandable way. Thank you to Fred Grine for assisting in obtaining my sample of cuboids from the AMNH and for your very positive comments on this project when it was just my final paper for Human Evolution. Also, thank you for supporting my decision to turn this project into a Master's Thesis and for agreeing to be my committee chair.

Finally, I want to thank all of my fellow IDPAS students for their advice and support throughout my time here at Stony Brook. It hasn't always been easy, but the level of camaraderie and everyone's genuine desire to help has made this experience so unforgettable. I would especially like to thank Peter Fernandez, Stephanie Maiolino, Evelyn Pain, and Kyle Viterbo, who each, in different ways, helped me to complete this thesis.

Introduction

Physical anthropologists continue to debate the nature of human locomotor evolution, including the reconstruction of locomotor behavior in the human-chimpanzee last common ancestor (LCA). Many hypotheses have been proposed, reflecting the frequent changes in our view of primate evolution (Richmond et al., 2001). Some of the earliest theories postulated a hylobatid-like ancestor, suggesting that the LCA was a small bodied, arboreal biped whose locomotion included a significant climbing component. Others advocated that humans evolved from a more primitive, monkey-like primate that exhibited above-branch quadrupedal locomotion (Morton, 1926; Straus, 1949). Most researchers today dismiss these hypotheses, and instead support the theory that the LCA was essentially African ape-like (Richmond et al., 2001; Harcourt-Smith and Aiello, 2004). According to this model, the LCA was an antipronograde climber with locomotion similar to that seen in African apes when traveling arboreally, and may have also included some knuckle walking behavior. Analyses of early hominin morphology and biomechanical studies have provided support for this hypothesis to the exclusion of others (Richmond et al., 2001).

Research that focuses on better understanding the morphology of the human and non-human primate foot has played an important role in these debates. Most scholars have argued that the human foot evolved from an African ape-like ancestor (Richmond et al., 2001; Harcourt-Smith and Aiello, 2004). Morton (1935) proposed that the foot of the LCA was essentially similar to a gorilla, allowing for grasping, but with some adaptations for bipedal weight bearing. More recent models agree that the foot was African ape-like, but differ in the details of how the foot evolved from this state to a more human-like configuration (Lewis, 1989; Kidd, 1999). Comparisons of the available fossil hominin foot bones have demonstrated general agreement

with this model, reporting the presence of many African ape-like features in the tarsal bones of extinct hominins (Sarmiento and Marcus, 2000; Harcourt-Smith, 2002; Berillon, 2004; Jungers et al., 2009). In contrast to these studies, recent analyses of the foot elements attributed to the new species *Ardipithecus ramidus* have suggested that specialized hominin locomotor adaptations evolved from a more primitive, monkey-like foot (Lovejoy et al., 2009). Specifically, adaptations in the *A.ramidus* foot have been used to propose an ancestor adapted for careful climbing and above-branch quadrupedal locomotion with plantigrade foot posture.

The holotype of *A.ramidus* (originally named *Australopithecus ramidus),* a set of associated teeth, was first discovered in 1993 (White et al., 1994). Subsequent finds in the following years yielded a large body of fossil material attributable to *A.ramidus,* including crania and numerous postcranial elements. All *A.ramidus* specimens come from the Middle Awash region of Ethopia, specifically in Aramis localities 1-7, and are dated to 4.4 Ma (White et al., 1994; White et al., 2009). At the time of its discovery, *A.ramidus* was the earliest known potential stem hominin, predating *Australopithecus anamensis* by 0.4 Ma (White et al., 1994). This species was initially placed in the hominin clade due to its modified C/P3 honing complex, anteriorly placed foramen magnum, and proximal ulnar morphology similar to later species of *Australopithecus* (White et al., 1994). Subsequent analyses of *A.ramidus* postcrania have suggested that this species was a terrestrial biped whose locomotion was more primitive than that seen in *Australopithecus* species (White et al., 2009).

The cuboid of *A.ramidus* figures prominently in Lovejoy et al.'s (2009) description and functional interpretation of locomotor behavior in the LCA. The authors hypothesize that changes in the foot morphology of African apes, including the loss of the *os peroneum*, a sesamoid bone in the *peroneus longus* tendon, and proximodistal shortening of the cuboid, led to

a derived re-orientation of *peroneus longus* as it crosses the plantar surface of the foot from lateral to medial. This tendon passes more parallel to the cuboid-metatarsal joints in extant great apes, while in humans and other hominins it crosses the foot more obliquely (Swindler and Wood, 1973; Lovejoy et al., 2009). In primates, *peroneus longus* serves to evert the foot and to resist inversion (Gray and Basmajian, 1968; Stern and Susman, 1983; Boyer et al., 2007; Lovejoy et al., 2009). Additionally, it may assist in the adduction of the hallux in non-human primates (Lovejoy et al., 2009, but see Boyer et al., 2007 for an opposing view). Lovejoy et al. (2009) propose that the orientation of *peroneus longus* has different functional implications in monkeys, apes, and humans. They assert that in great apes, the parallel orientation allows for more midfoot laxity, which is useful for grasping a substrate during climbing. While in both Old World monkeys and humans, the opblique *peroneus longus* orientation creates a more rigid midfoot. Furthermore, Lovejoy et al. (2009) suggest that it also supports the longitudinal arches in humans, and therefore may be related to the development of modern bipedality (Lovejoy et al., 2009; Ward et al., 2011).

Based on qualitative observations of the orientation of the *peroneus longus* groove in *A.ramidus*, Lovejoy et al. (2009) suggest that the tendon crossed the foot obliquely, similar to the orientation seen in Old World monkeys. As *A.ramidus* is positioned so close to the base on the hominin tree, this indicated to the authors that the human-chimpanzee LCA also shared an oblique orientation. This observation, along with the analysis of further characters of the *A.ramidus* foot, led them to conclude that the LCA was more monkey-like than had been previously thought. Unfortunately, no quantification of the *peroneus longus* tendon orientation was provided in Lovejoy et al.'s descriptions of *A.ramidus*, and it remains unclear how its cuboid morphology is similar to or different from other primates.

The goal of this study was to quantify the angle of *peroneus longus* relative to the distal articular facet for the fourth metatarsal (MT4) in order to evaluate the hypotheses put forth by Lovejoy et al. (2009). To draw conclusions about the locomotor behavior of fossil species based on the *peroneus longus* tendon orientation, it must be possible to distinguish extant primate groups based on this morphology. Therefore, I first tested the hypothesis that there are significant differences in groove orientation among primate taxa. Based on the conclusions reached by Lovejoy et al. (2009), I predicted that the groove for *peroneus longus* would be more obliquely oriented in humans and monkeys and more parallel in apes. Second, I tested the hypothesis that *A.ramidus* was more similar to a monkey than a great ape, predicting its groove orientation would be more oblique. In addition to specific quantification of the *peroneus longus* groove, I also analyzed the overall morphology of the distal cuboid using 3D geometric morphometrics in order to better understand how the cuboid as a whole differs among taxaonomic and functional groups.

Materials and Methods

This study quantified the angle of the *peroneus longus* groove and the morphology of the distal cuboid in a comparative sample of 54 *Homo sapiens* and 228 extant non-human primates, as well as in a sample of fossil apes and hominins, including *Oreopithecus bambolii, Proconsul heseloni, Sivapithecus spp., Ardipithecus ramidus, Homo habilis*, and *Homo floresiensis* (Table 1). The cuboids used in this study were borrowed from the American Museum of Natural History, the Museum of Comparative Zoology at Harvard University, and the Stony Brook University Museum. Additional cuboids were analyzed from 3D images of computed tomography scans from the National Museum of Natural History, and Academy of Natural

Sciences, Philadelphia. Fossil cuboids were quantified from 3D scans of the original bones or casts. Finally, data for *A.ramidus* were taken from a polygon model derived from microCT scan data, graciously provided by Tim White and Gen Suwa.

For each cuboid, I took seven landmarks that provided x, y, z coordinates that could then be used to reconstruct the cuboid morphology. Landmarks on physical bones were obtained using a MicroScribe M 3D digitizer (Revware Systems, Inc). The same eight landmarks were taken from 3D images using the freeware program 3D Tool (www.3D-tool.de). Landmarks were chosen to quantify both the angle of the groove for *peroneus longus*, located towards the distal end of the plantar side of the cuboid, and the morphology of the distal articular facet for the fourth and fifth metatarsals (MT4 and MT5). A size proxy was calculated from landmarks 1 – 5, which approximated the surface area of the distal articular facet for MT4 and MT5. Some of the landmarks used in this study are equivalent to those used by Harcourt-Smith (2002) in his PhD dissertation, while others were created specifically for this project. Table 2 describes the location of each landmark, and landmark locations are illustrated in Figure 1.

Calculation of the angle of the *peroneus longus* groove was done in MatLAB using code written by Caley Orr. This code calculates the groove angle relative to the distal articular facet for MT4, as this approximates the position of the bone while articulated in the foot. First, the points are placed into a standard coordinate frame and rotated to normalize for differences in side. A midpoint is taken between landmarks 4 and 7, and a line is drawn between this midpoint and landmark 6. This provides a vector representing the orientation of the groove (Figure 1). As the *A.ramidus* cuboid is broken at landmark 1, the orientation of the articular facet for MT4 was calculated by placing a plane on top of the distal articular surface using landmarks 2, 3, and 5, from which a vector is calculated. The resulting angle between this vector and the groove vector

represents the orientation of the *peroneus longus* groove. A large angle indicates a more obliquely set groove, while a small angle indicates a parallel groove.

Due to the elimination of landmark 1 in the calculation of the reference plane, all of the platyrrhine specimens were reconstructed as having negative angles. This is likely an artifact of a difference in morphology in these individuals, in which the medio-dorsal corner (location of landmark 2) has a distinctive lip elevated above the level of the articular facet. This results in a skewed orientation of the plane used for comparison with the groove, rotating the cuboid into a position that is not reflective of its orientation when articulated. Because of this error, all platyrrhine cuboids were redigitized using an alternate location for landmark 2 slightly inferior to the original point (Figure 2). Differences in groove angle between genera and locomotor categories were assessed using ANOVA with Tukey Honest Significant Difference post-hoc tests in SPSS 17.0. Taxa included in each locomotor category are shown in Table 3.

The 3D geometric morphometric study was conducted using the same landmarks described above. In the case of platyrrhines, the original values for landmark 2 were used in order to more accurately represent the overall morphology of the cuboid. Data were superimposed using generalized Procrustes analysis (GPA), which removes differences in the landmark data due to orientation, translation, and centroid size (Rohlf and Slice, 1990). Principal components analysis (PCA) was used to investigate variation in the data set. Both GPA and PCA were performed in Morphologika2 v. 2.5. Analyses were run twice, once using an estimated point for landmark 1 in *A.ramidus*, and once eliminating that data point and using only the other six landmarks. A correlation of the principal component (PC) scores for each individual PC showed that the results of both methods were statistically indistinguishable for the first six PCs ($p<0.0001$). Therefore, only the results using the full seven landmark set are presented for these

PCs. There were significant differences between the two methods on PC 7, so results from both will be presented.

Allometric correlations were investigated on individual PCs in R 2.14.1 by regressing PC scores on the logarithm of centroid size, which is calculated as the square root of the sum of squared differences from each landmark to the centroid (the geometric center of all the landmarks for a particular individual) (Rohlf and Slice, 1990; Baab, 2008). Differences among taxonomic groups along particular PCs were analyzed in SPSS using MANOVA with Tukey post-hoc tests. Similarities between fossils and extant species were assessed using pairwise Procrustes distances, which refer to the distance between two landmark configurations in Kendall's shape space (Slice, 2001).

A study of measurement error was conducted in order to assure the accuracy and repeatability of the groove angle calculation. All seven landmarks were taken once per week for five weeks on randomly selected *H.sapiens, Pan,* and *Macaca* cuboids. These measurements were compared by calculating the angle for the *peroneus longus* groove for each week and comparing the five results. Additionally, a qualitative rank analysis was conducted independently by three observers (Erin Achilles, Biren Patel, and Caley Orr). We visually ranked the orientation of the *peroneus longus* groove from the most parallel to the most oblique in 12 *H.sapiens*, 10 *Pan troglodytes.,* and 10 *Nasalis larvatus.* The results of this qualitative assessment were compared using a Spearman's Rho correlation to determine if there was a difference between observers using qualitative assessments. Qualitative assessments were also compared with the results from the quantitative study to see if there were differences in the two types of assessment.

Results

Groove Orientation

Results of the error study indicated that there was less than 5% error in angle measurement. Therefore, groove angle is a robust measurement and is repeatable. Results of the qualitative rank analysis were not significant (Spearman's Rho: $p>0.05$), indicating that there was no correlation between rankings of groove angle from most parallel to most oblique among the three observers. Therefore, qualitative assessment of the cuboid is not a reliable measure of groove orientation. When comparing the qualitative measurements with ranks obtained from quantitative angle measurements, the result was also not significant (Spearman's Rho: $p>0.05$). This is further evidence suggesting that qualitative assessment of groove angle does not accurately represent the morphology present on the cuboid.

In order to determine if body size played a role in the orientation of the groove, groove angle for each individual was regressed against a size proxy variable calculated using the distal articular facet of the cuboid. Results of the linear model indicate a significant correlation between groove angle and size of the cuboid ($p<0.05$, t=-2.221). However, the R^2 value of 0.02 is very low, suggesting that this relationship is unlikely to be meaningful (Figure 3). Therefore, any observed differences in groove angle are not due to differences in size.

Results of the analysis of angle measurement are summarized in Table 4. In order to determine if individual taxa differed significantly, I first compared closely related genera within superfamilies. Though the results of the ANOVA comparing cercopithecid genera indicated that there was significant variation among the genera ($p<0.05$, $F=2.587$, $df=7$), post-hoc tests indicated no specific, significant pair-wise differences. A T-test comparing the two platyrrhine genera (*Ateles* and *Alouatta*) showed no significant difference between the two ($p=0.085$,

t=1.818, df=19). An ANOVA indicated that hominoid genera were significantly different (p<0.0001, F=20.360, df=3) and post-hoc tests revealed that this difference was driven by *Hylobates*, which has a significantly more oblique groove than *Pan, Gorilla,* and *Pongo* (p<0.0001 for all pairwise comparisons). Based on these results, I used ANOVA to compare atelids, cercopithecids, great apes, *Hylobates*, and *H.sapiens*. Results of this analysis showed significant differences in groove angle among these groups (p<0.0001, F=34.474, df=4, Figure 4). Post-hoc tests revealed that all groups were significantly different, with the exception of *H.sapiens* and cercopithecids (Table 5). However, despite these differences, there was a large range of variation within each category, especially within *H.sapiens*.

Figure 5 shows groove orientation separated by general locomotor categories: arboreal quadrupeds, terrestrial quadrupeds, brachiators, quadrumanous climbers, knuckle walkers, and bipedal taxa. There were significant differences between locomotor categories (p<0.0001, F=14.740, df=5). Results of the post-hoc tests for significance are shown in Table 6. The brachiating group, which includes *Hylobates,* was significantly different from all other locomotor groups. The quadrumanous climber group, which includes *Pongo,* was significantly different from all quadrupeds, but not the other large-bodied apes (knuckle-walkers and bipeds). *H.sapiens* was only significantly different from brachiators, while both arboreal and terrestrial quadrupeds were different from brachiators, quadrumanous climbers, and knuckle-walkers. Again, however, each of these locomotor groups exhibited a large range of variation in groove angle.

When comparing groove angle in extant primates to fossil species, all hominin species (*A.ramidus, H.habilis, H.floresiensis)* fell well within the range of *H.sapiens* and had a relatively oblique groove (Figure 4). However, they also fell within the range of *Hylobates*, cercopithecids,

and at the higher end of the great ape range. The fossil ape *Sivapithecus* also fell within these ranges. In contrast, *Oreopithecus* had a very parallel groove, falling towards the lower end of the *Gorilla* distribution and within the atelid range. *Proconsul* fell very near the median great ape value, but also overlaped with the other taxaonomic groups. The individual in the sample with the most similar groove angle to *A.ramidus* was *Mandrillus sphinx* 34090, followed by *H.sapiens* AS-25 from the collection at Stony Brook University.

3D Geometric Morphometric Analysis

Based on the results of the principal components analysis, the scores on PCs 1 – 7 were used in subsequent analyses, as they were clearly interpretable. Regressing PC scores on log centroid size showed that PCs 1 – 4 had significant allometric correlations (PC 1: $p<0.0001$, $R^2=0.08$; PC2: $p<0.0001$, $R^2=0.10$; PC3: $p<0.0001$, $R^2=0.26$; PC4: $p<0.01$, $R^2=0.03$). However, the R^2 values for all of these were relatively small, particularly on PCs 1, 2, and 4, suggesting that cuboid size, which is likely to be correlated with body mass, does not play a large role. Though the R^2 value for PC 3 was somewhat larger (0.26), this was largely driven by *H.sapiens*, which are similar in size to the great apes but have higher PC 3 scores.

Results of the MANOVA showed significant differences between taxonomic groups on all of the first seven principal components ($p<0.0001$ for all components; Table 7). The first principal component accounted for 24% of the overall variance in the sample of 289 cuboids. This axis captured variation in groove angle, with higher scores indicating a more obliquely set groove (Figure 6). Here, the great apes and atelids were clearly differentiated from other taxonomic groups, particularly *Hylobates*, due to their more parallel groove orientation. *H.sapiens* was significantly different from all other groups on PC 1, but plotted close to some of

the cercopithecines, primarily those from the genus *Macaca.* Both of these groups, as well as hylobatids, had more obliquely oriented grooves. Other cercopithecines and colobines have a large range of variation on the plot, suggesting a groove morphology that is intermediate between the great apes/atelids and *H.sapiens*/*Hylobates. A.ramidus* fell very near to the center of the plot on PC 1.

PC 2, which captured 19% of the total variance, primarily described variation in the location of landmark 5, with higher values indicating a distal articular surface that is projected more distally at the point where the facets for MT4 and MT5 meet on the plantar side (Figure 6). All apes, including *H.sapiens*, are grouped to the exclusion of cercopithecine monkeys by this PC, as they have a more projected surface at this location. Though *Pan* was significantly different from the other apes, it fell close to them on the PC plot, with the exception of some individuals with very high PC scores. Cercopithecines, with a distal articular surface that was less projecting on the plantar side, were further distinguished from colobines and atelids by this PC. As with PC 1, *A.ramidus* fell toward the middle of the plot.

Principal components 3 and 4 accounted for 12% and 9% of the variance, respectively. PC 3 described differences in the size of the distal articular facets for MT4 and MT5, with larger scores indicating a smaller surface for MT5. PC 4 accounted for changes in the most laterally projecting point of the articular facet for MT5 (location of landmark 4), which is more proximal in individuals with low PC scores. This led the articular surface for MT5 to be sloped proximally, as opposed to the more flat condition seen in individuals with high PC scores. Both of these PCs clearly distinguished *Hylobates*, which has a large, flat articular surface for MT5. PC 3 also showed a statistically significant difference between *H.sapiens* and all other taxonomic

groups, but the range of variation within this group overlaps with all other taxa. Again, *A.ramidus* exhibited an intermediate score on both of these axes.

PCs 5 and 6 accounted for 7% and 5% of the variance, respectively. PC 5 mainly accounted for the variance seen in atelids, which have a distinct projection of bone at the medio-dorsal corner of the distal articular facet (the location of landmark 2). *Hylobates* was also distinct on this PC, lacking the projecting surface seen in atelids. *A.ramidus* once again fell towards the middle of the plot. PC 6 accounted further for differences in the location of landmark 4: lower PC scores indicated a more dorsal orientation of the most lateral point of the MT5 facet (Figure 7). Though difficult to see from the plot, this PC statistically separated atelids and *Pongo* from cercopithecids. Notably, *A.ramidus* had a high PC 6 score, indicating that the lateral-most point of the distal articular facet for MT5 is angled toward the plantar side of the bone.

Finally, PC 7 explained 5% of the overall variance in the data. For the data set including landmark 1 (estimated for *A.ramidus*), PC 7 separated out *Pongo*, which had a PC low score and was significantly different from all other taxa. This PC captured differences in the location of landmarks 1 and 2, with a low score indicating a more laterally placed medio-plantar corner to the distal articular facet for MT4. *A.ramidus* had the highest PC 7 score, indicating a very medial placement of the medial-plantar corner of the facet. However, this may be due to inaccuracies in the estimated placement of landmark 1 in *A.ramidus.* For the data set excluding landmark 1, the variation at this landmark seen in *Pongo* is no longer captured and this taxon is only significantly different from colobines. *A.ramidus* still has a very high PC score on this axis, suggesting that some additional differences in morphology other than those at the medio-plantar corner are being captured by this PC. However, due to the missing landmark on *A.ramidus*, we must be cautious in the interpretation of PC 7.

An analysis of the pairwise Procrustes distances generated by the PCA showed that *A.ramidus* was most similar in overall shape to *Papio* specimen 239743, followed by *Gorilla* specimen 54355. Figure 8 shows the pairwise Procrustes distances for *A.ramidus* as compared to the major taxonomic groups. *A.ramidus* is most similar to cercopithecids. *H.habilis* and *Oreopithecus* are both more similar to *H.sapiens* and hominoids, while *H.floresiensis* was most similar to cercopithecids and *H.sapiens*. *Proconsul* and *Sivapithecus* were most similar to cercopithecids.

Discussion

The results of this study indicate that some taxonomic groups can be discriminated by the angle of the groove for *peroneus longus.* For the most part, genera cannot be distinguished based on groove morphology, with the exception of *Hylobates*, which has a very oblique orientation. However, groove morphology does separate groups at higher taxonomic levels: great apes and atelids both have relatively parallel grooves, with atelids having the most parallel morphology. *H.sapiens* and cercopithecids are very similar in their groove orientation, falling intermediate between great apes/atelids and *Hylobates*. The same pattern was recovered in the geometric morphometric analysis, in which PC 1 captured variation in groove angle. Great apes and atelids group together on this PC, exhibiting more parallel groove morphology, while *H.sapiens* and cercopithecids have more oblique grooves. These results support the conclusions of Lovejoy et al. (2009) in that it is possible to discriminate some taxonomic groups using this metric.

This study also supports the conclusion of Lovejoy et al. (2009) that *H.sapiens* and cercopithecids have a similar, obliquely oriented groove angle, in contrast to the parallel groove seen in great apes. Lovejoy et al. (2009) used this as support that the LCA of humans and

chimpanzees was not great ape-like, and instead suggested that *H.sapiens* retained their oblique groove morphology from a more monkey-like ancestor. However, it is important to note that the median groove angle is not very different between the great apes and *H.sapiens,* and there is significant overlap among all of the groups. Though it is possible to conclude that this is a plesiomorphic trait shared by *H.sapiens* and Old World monkeys, it is just as likely that this similarity in morphology is due to a subsequent reversal in *H.sapiens.* In contrast to the results from the angular measurement study, *H.sapiens* and cercopithecids do have significantly different groove morphology in the geometric morphometric analysis. This may further suggest that groove angle is not homologous in these species. Conversely, the grouping of non-human great apes along PC 1, as well as the grouping of all apes along PC 2, is support for an ape-like ancestral condition. Additionally, analysis of the available fossil material calls the polarity of this trait into question. *Proconsul* and *Oreopithecus* both possess a relatively parallel groove, as do atelids. If this is the ancestral state, it suggests that cercopithecids are derived in their groove angle morphology, and hominids (excluding the more derived *H.sapiens*) retain the plesiomorphic groove morphology. As the range of variation within all groups is quite large, it is likely that this is a relatively labile trait that may have changed often over the course of evolutionary time, making assessment of the ancestral state difficult.

Though we are able to distinguish taxonomic groups based on groove morphology, the application of this method for determining locomotor pattern is more difficult. Though there were some differences in groove angle among locomotor categories, these differences are more likely reflective of phylogenetic relatedness as opposed to locomotor similarity. As the locomotor categories used in this study almost correspond to the taxonomic groupings, we cannot draw any strong conclusions about the relationship between groove angle and locomotor

pattern. In fact, the clear difference between atelids and *Hylobates* in groove angle suggests that this metric is not a good indicator of locomotor behavior. As atelids are semi-brachiators, we would expect them to have a similar groove angle to *Hylobates*, but the results of both the angular study and the geometric morphometric analysis suggest that these two groups are quite different. Therefore, it is likely that this metric is not an appropriate means with which to assess locomotor behavior in either extant or extinct species.

In support of the conclusions of Lovejoy et al. (2009), there is some indication that the groove angle in *A.ramidus* is obliquely oriented. Further, its groove angle is most similar to that of a monkey, and its overall cuboid morphology as measured by Procrustes distance is more monkey-like than ape-like. However, the angle seen in *A.ramidus* is also very similar to that seen in *H.sapiens*. If this trait is functionally linked to producing a more rigid midfoot, it is just as likely that the morphology seen in *A.ramidus* indicates a derived adaptation to bipedal locomotion rather than plesiomorphic retention from a pronograde, quadrupedal ancestor. On the other hand, *A.ramidus* falls within the range of great ape variation, so the presence of a "chimp-like" morphology cannot be ruled out for this species. Another aspect of cuboid morphology that may tie *A.ramidus* to the great apes is the *os peroneum*, the sesamoid bone found in the *peroneus longus* tendon. Though a facet for this sesamoid is said to be present on the *A. ramidus* cuboid, qualitative observation of this bone does not definitely show this facet to be present. Further support for the idea that the LCA could have been ape-like in midfoot function comes from the angle seen in *Proconsul*, which is nearly identical to the great ape median. As *Proconsul* is considered to be one of the earlier hominoids, this indicates that as far back as the early Miocene, fossil primates may have had an "ape-like" morphology to the *peroneus longus* groove.

It is important to note the extreme range of variability in groove angle seen in this sample, in particular in *H.sapiens.* Additionally, *H. sapiens* tends to occupy a large portion of the shape space in the geometric morphometric analysis. This variability makes it difficult to confidently align the morphological affinities of the *A.ramidus* cuboid with any particular species or locomotor group. As we only have one cuboid from *A.ramidus* for comparison, it is quite possible that it is not representative of the species as a whole. The amount of variability in the extant sample makes it even more likely that this one cuboid does not represent the average condition in all members of the species. Further, as locomotor behavior is difficult to assess with this metric, caution is urged in interpreting the biomechanics of the midfoot in *A.ramidus* based on this particular character, and retrodicting the locomotor behavior in the last common ancestor based on groove angle in *A.ramidus* is not warranted. Therefore, the conclusions drawn by Lovejoy et al. (2009) about locomotion in *A.ramidus* and the human-chimpanzee LCA should be re-evaluated.

Results of the principal components analysis for PCs 2 – 7 do not add greatly to the discussion of the status of the LCA. *Hylobates* is consistently unique on the PC ordinations, apart from PC2, where it falls with the other apes. This may be related to a secondary differentiation in hylobatids, which led to their unique locomotor pattern and morphology. As *Hylobates* was isolated during the Pleistocene (Whittaker et al., 2007), it is likely that it rapidly speciated and underwent changed in morphology, possibly leading to changes in its cuboid. PC 5 distinguishes the unique projecting morphology of the medio-dorsal corner of the distal articular facet seen in atelids, which is likely a derived trait within this taxon. Finally, PC 7 separates *Pongo* from the other taxa, suggesting that this group possesses a uniquely derived lateral placement of the medio-plantar corner of the distal articular facet. The functional significance of these traits is

unknown, but as they are apomorphies of particular genera, they do not have bearing on questions of evolutionary relationships.

The affinities of *A. ramidus* are also difficult to discern from the geometric morphometric analysis. In almost every case, *A.ramidus* falls directly in the middle of the plot, suggesting that it likely shared traits with monkeys, apes, and humans, as well as possessed some unique features. This trend toward a generalized morphology is exemplified by a review of the pairwise Procrustes distances, which show that although *A.ramidus* is most similar to cercopithecids, it also falls close to members of all other taxonomic groups. Additionally, it is difficult to accurately assess the placement of *A.ramidus* due to the missing landmark. Therefore, we should use caution when drawing conclusions about the relationship of this species to other taxa; it is likely that the cuboid is not the best means with which to assess of the affinities of this species.

Though this study partially supports the conclusions of Lovejoy et al. (2009) in that some taxa can be differentiated using *peroneus longus* groove morphology, and that *A.ramidus* shares similarities with monkeys, we must be cautious in using groove angle to interpret locomotor patterns. There is a huge range of variability in cuboid morphology within groups, suggesting that it is impossible to draw firm conclusions about potential locomotor behavior in fossil species. As groove angle is highly variable, both within and among groups, it is not possible to assess to the polarity of this trait; we cannot know for sure what the ancestral state was, or whether or not *H.sapiens* inherited its morphology from a monkey-like ancestor. Therefore, the results of this study suggest that the cuboid bone should not be used to make inferences about LCA, and the conclusions reached by Lovejoy et al. (2009) that relate to this bone should be reconsidered.

References

Baab, K.L., 2008. The taxonomic implications of cranial shape variation in *Homo erectus*. J Hum Evol 54, 827-847.

Berillon, G., 2004. In what manner did they walk on two legs?: An architectural perspective from the functional diagnostics of the early hominid foot, in: Meldrum, D.J., Hilton, C.E. (Eds.), From biped to strider: The emergence of modern human walking, running, and resource transport. Kluwer Academic/Plenum Publishers, New York.

Boyer, D.M., Patel, B.A., Larson, S.G., Stern, J.T., 2007. Telemetered electromyography of peronus longus in *Varecia variegata* and *Eulemur rubriventer*: Implications for the functional significance of a large peroneal process. J Hum Evol 53, 119-134.

Gray, E.G., Basmajian, J.V., 1968. Electromyography and cinematography of leg and foot ("normal" and flat) during walking. Anat Rec 161, 1-16.

Harcourt-Smith, W., 2002. Form and function in the hominoid tarsal skeleton, PhD Thesis. University College London, London.

Harcourt-Smith, W.E.H., Aiello, L.C., 2004. Fossils, feet and the evolution of human bipedal locomotion. J Anat 204, 403-416.

Jungers, W.L., Harcourt-Smith, W.E.H., Wunderlich, R.E., Tocheri, M.W., Larson, S.G., Sutikna, T., Due, R.A., Morwood, M.J., 2009. The foot of *Homo floresiensis*. Nature 459, 81-84.

Kidd, R., 1999. Evolution of the rearfoot: A model of adaptation with evidence from the fossil record. J Am Med Assoc 89, 2-17.

Lewis, O., 1989. Functional morphology of the evolving hand and foot. Claredon Press, Oxford.

Lovejoy, C.O., Latimer, B., Suwa, G., Asfaw, B., White, T.D., 2009. Combining prehension and propulsion: The foot of *Ardipithecus ramidus* Science 326, 72-72e78.

Morton, D.J., 1926. Evolution of man's erect posture (preliminary report). J Morphol 43, 147-179.

Morton, D.J., 1935. The human foot: It's evolution, physiology, and functional disorders. Columbia University Press, New York.

Richmond, B., Begun, D., Strait, D., 2001. Origin of human bipedalism: The knuckle-walking hypothesis revisted. Yearb Phys Anthropol 44, 71-105.

Rohlf, F.J., Slice, D., 1990. Extensions of the Procrustes method for the optimal superimposition of landmarks. Syst Zool 39, 40-59.

Sarmiento, E.E., Marcus, L.F., 2000. The *Os Navicular* of humans, great apes, OH 8, Hadar, and *Oreopithecus*: Function, phylogeny, and multivariate analysis. Am Mus Novit 3288, 1-38.

Slice, D.E., 2001. Landmark coordinates alligned by Procrustes analysis do not lie in Kendall's shape space. Syst Biol 50, 141-149.

Stern, J.T., Susman, R.R., 1983. The locomotor anatomy of *Australopithecus afarensis*. Am J Phys Anthropol 60, 279 - 317.

Straus, W.L., 1949. The riddle of man's ancestry. Q Rev Biol 24, 200-223.

Swindler, D.R., Wood, C.D., 1973. An atlas of primate gross anatomy: Baboon, chimpanzee, and man. University of Washington Press, Seattle.

Ward, C.V., Kimbel, W.H., Johanson, D.C., 2011. Complete fourth metatarsal and arches in the foot of *Australopithecus afarensis*. Science 331, 750-753.

White, T.D., Asfaw, B., Beyene, Y., Haile-Selassie, Y., Lovejoy, C.O., Suwa, G., WoldeGabriel, G., 2009. *Ardipithecus ramidus* and the paleobiology of early hominins. Science 326, 64-86.

White, T.D., Suwa, G., Asfaw, B., 1994. *Australopithecus ramidus*, a new species of early hominid from Aramis, Ethiopia. Nature 371, 306-312.

Whittaker, D.J., Morales, J.C., Melnick, D.J., 2007. Resolution of the *Hylobates* phylogeny: Congruence of mitochondrial D-loop sequences with molecular, behavioral, and morphological data sets. Mol Phylogenet Evol 45, 620-628.

Appendix

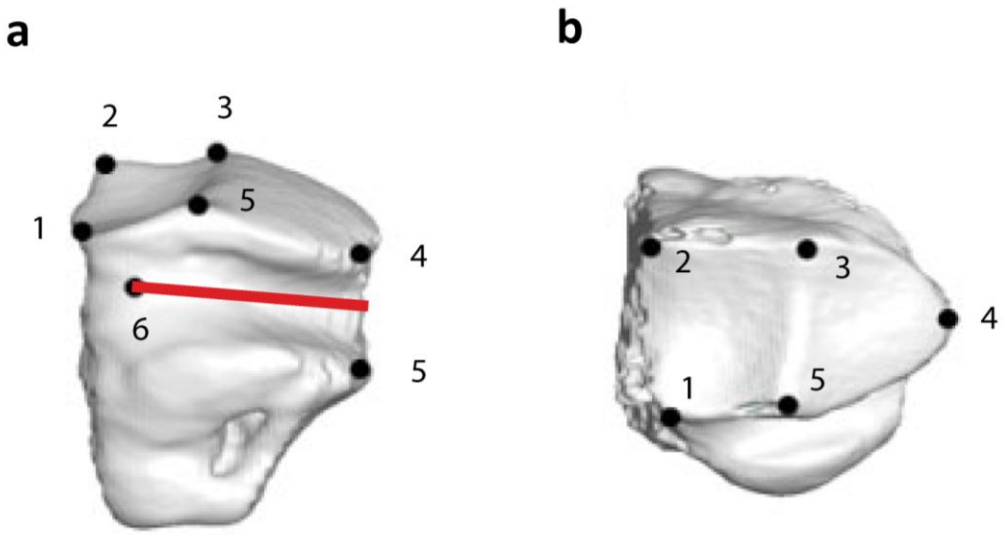

Figure 1: Location of landmarks shown on a gorilla cuboid. (a) plantar view; the red line represents the vector created to approximate the groove for *peroneus longus*, and (b) distal view.

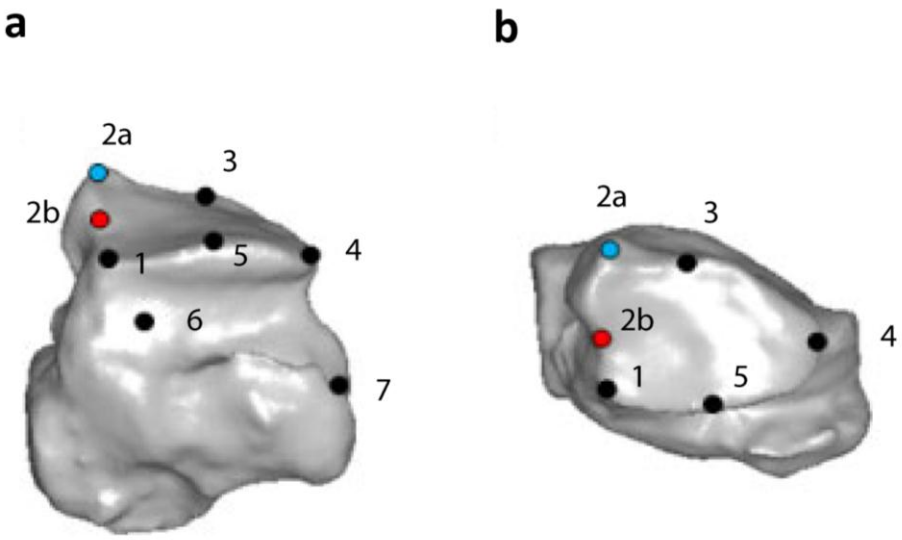

Figure 2: Location of landmarks for platyrrhine specimens shown on an *Alouatta* cuboid. The original landmark 2 is shown in blue. The new landmark 2 is shown in red. (a) plantar view and (b) distal view.

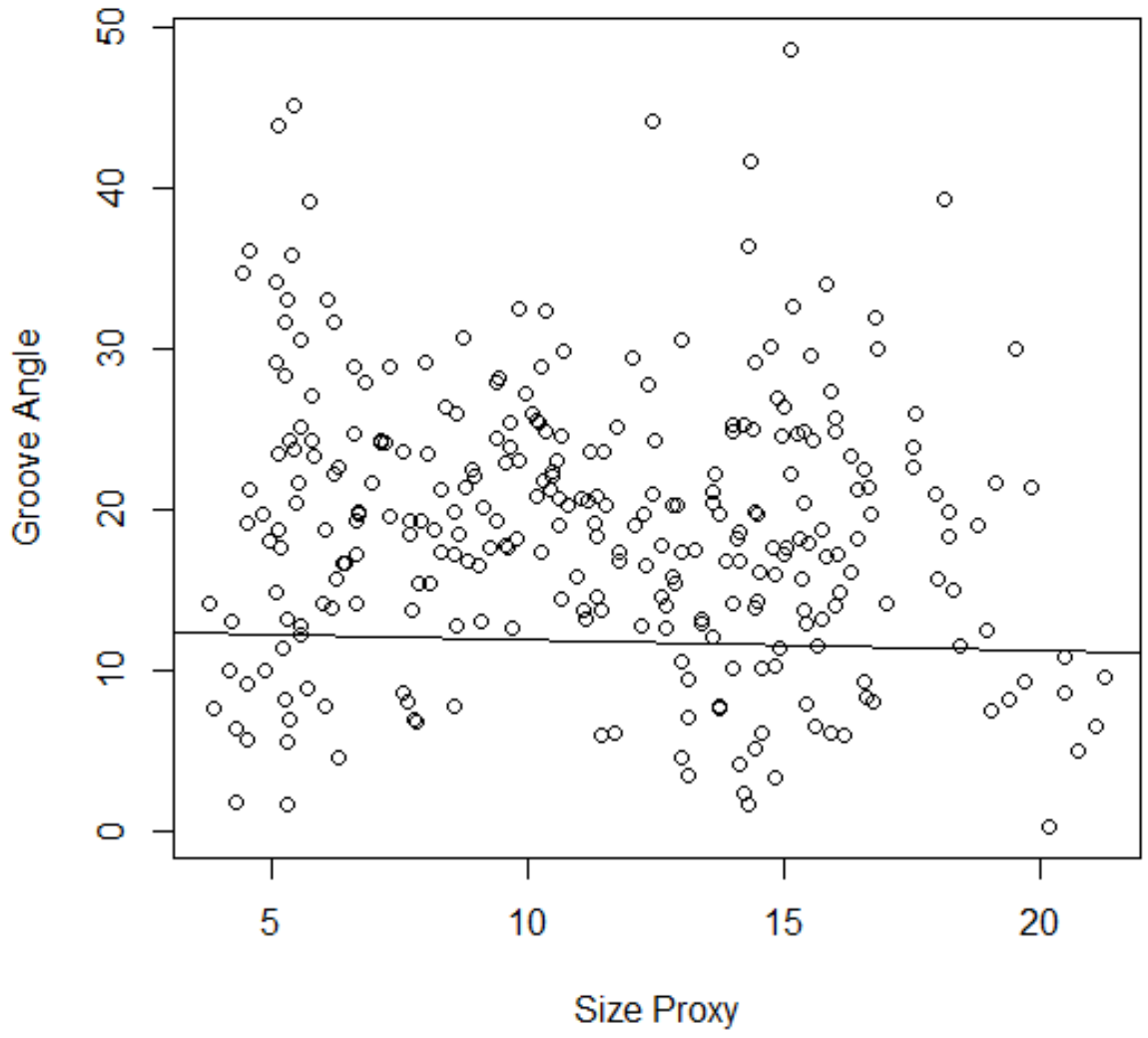

Figure 3: Scatterplot of size proxy vs. groove angle. The best-fit line is shown. R^2=0.02.

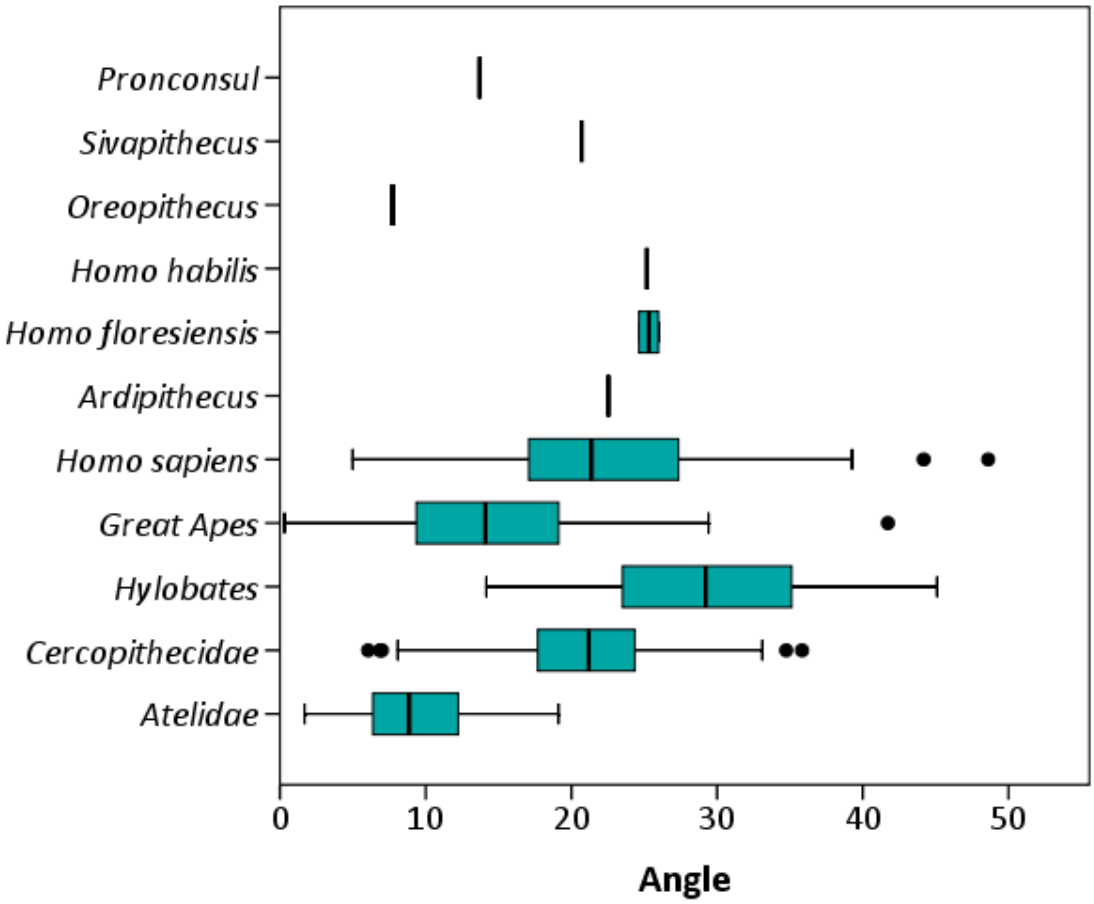

Figure 4: Boxplot showing groove angle measurement by taxon, including fossil species. Bars indicate median angle measurements. Error bars indicate full non-outlier range.

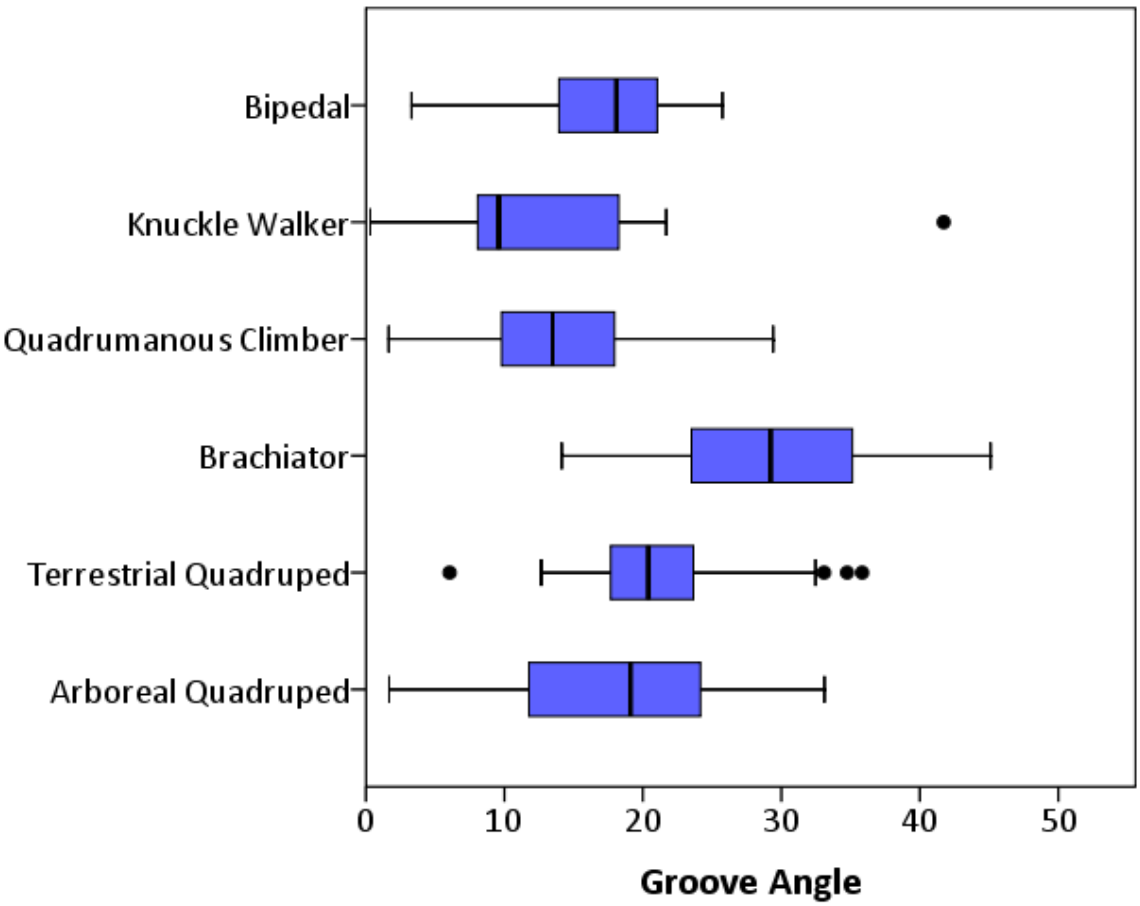

Figure 5: Boxplot showing groove angle measurement by general locomotor groups. Bars indicate median angle measurements. Error bars indicate full non-outlier range.

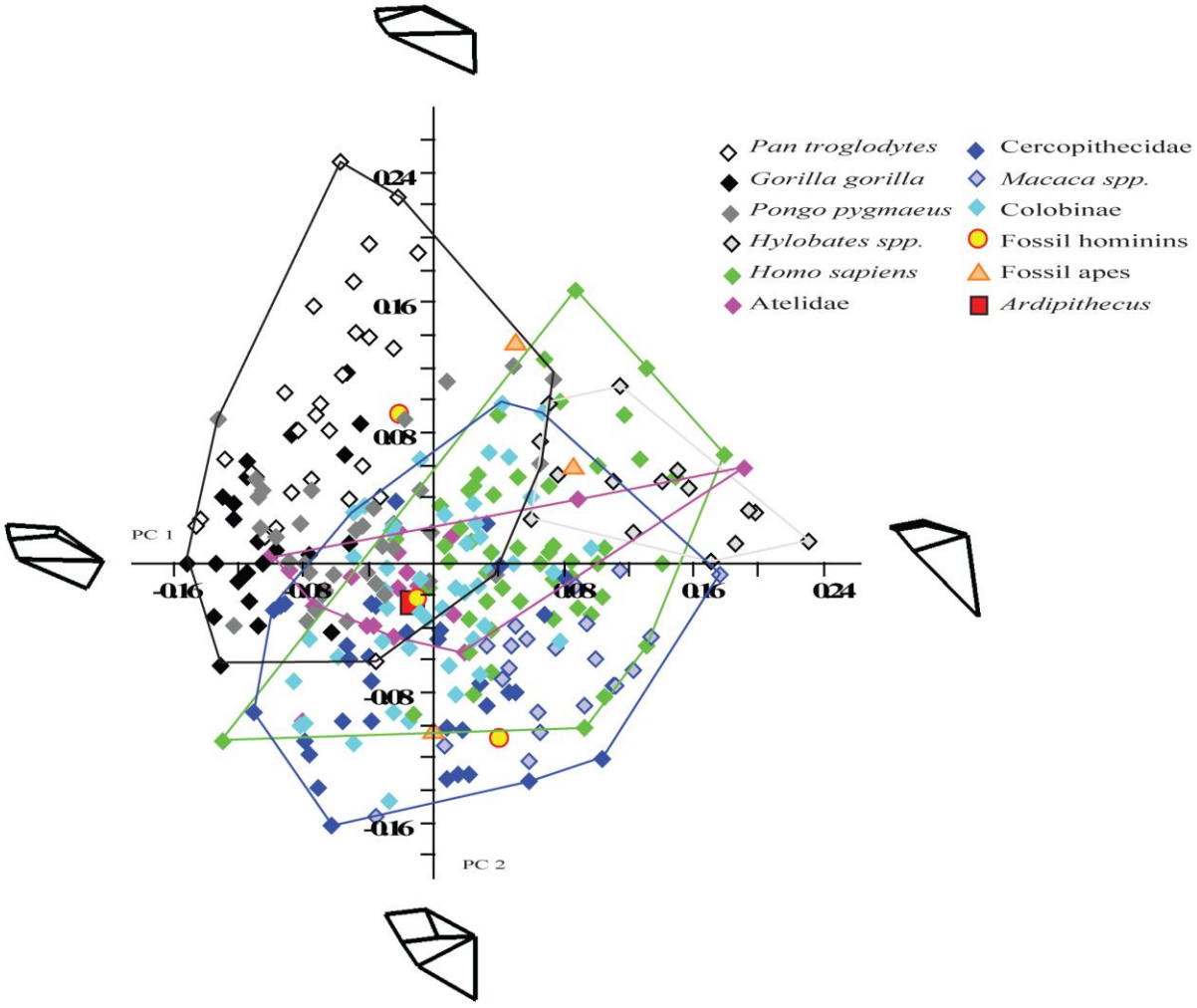

Figure 6: Principal component analysis of primate cuboids. PC 1 (24% of the variance) vs. PC 2 (19% of the variance). Minimum convex polygons are shown for great apes (black), hylobatids (grey), *Homo sapiens* (green), atelids (pink), and cercopithecids (blue).

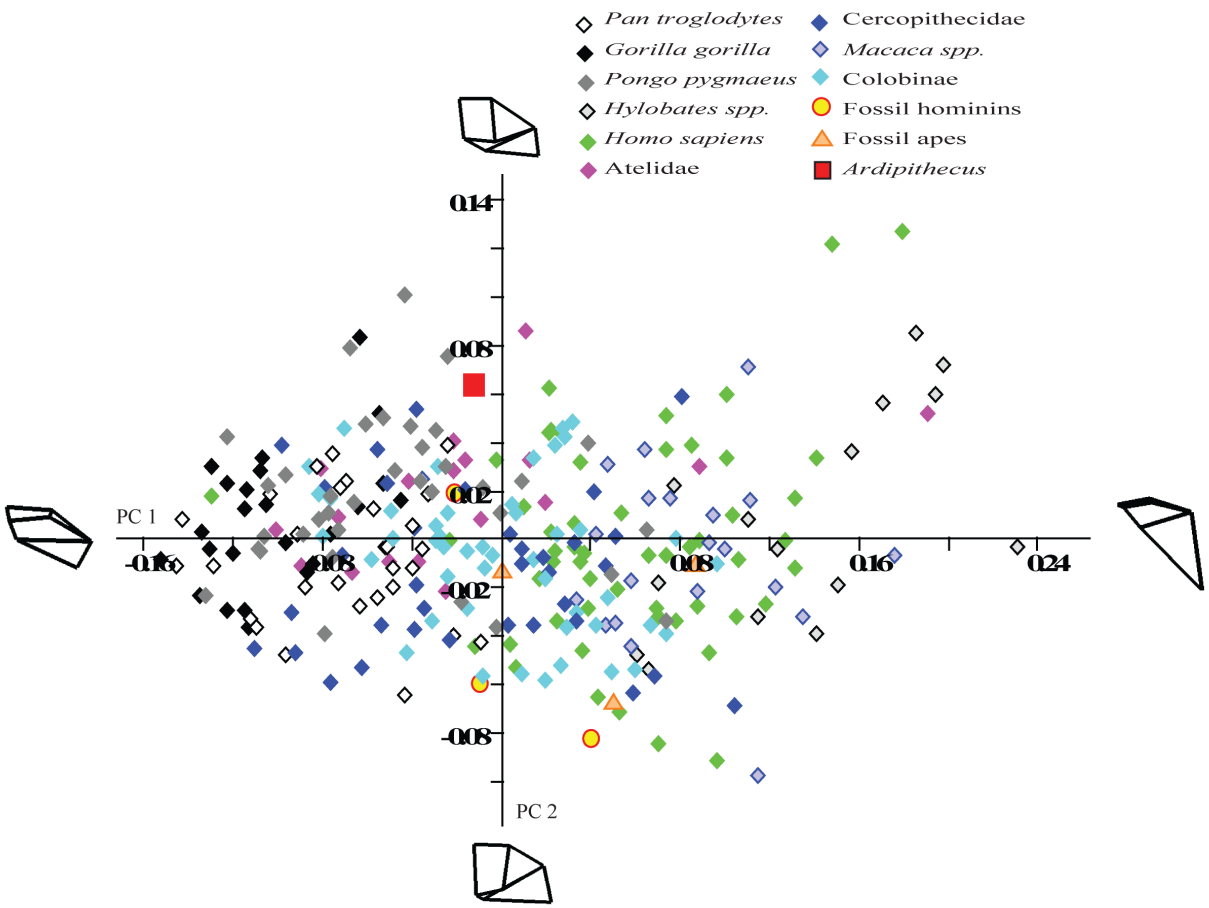

Figure 7: Principal component analysis of primate cuboids. PC 1 (24% of the variance) vs. PC 6 (5% of the variance). Note the placement of *Ardipithecus* (red square).

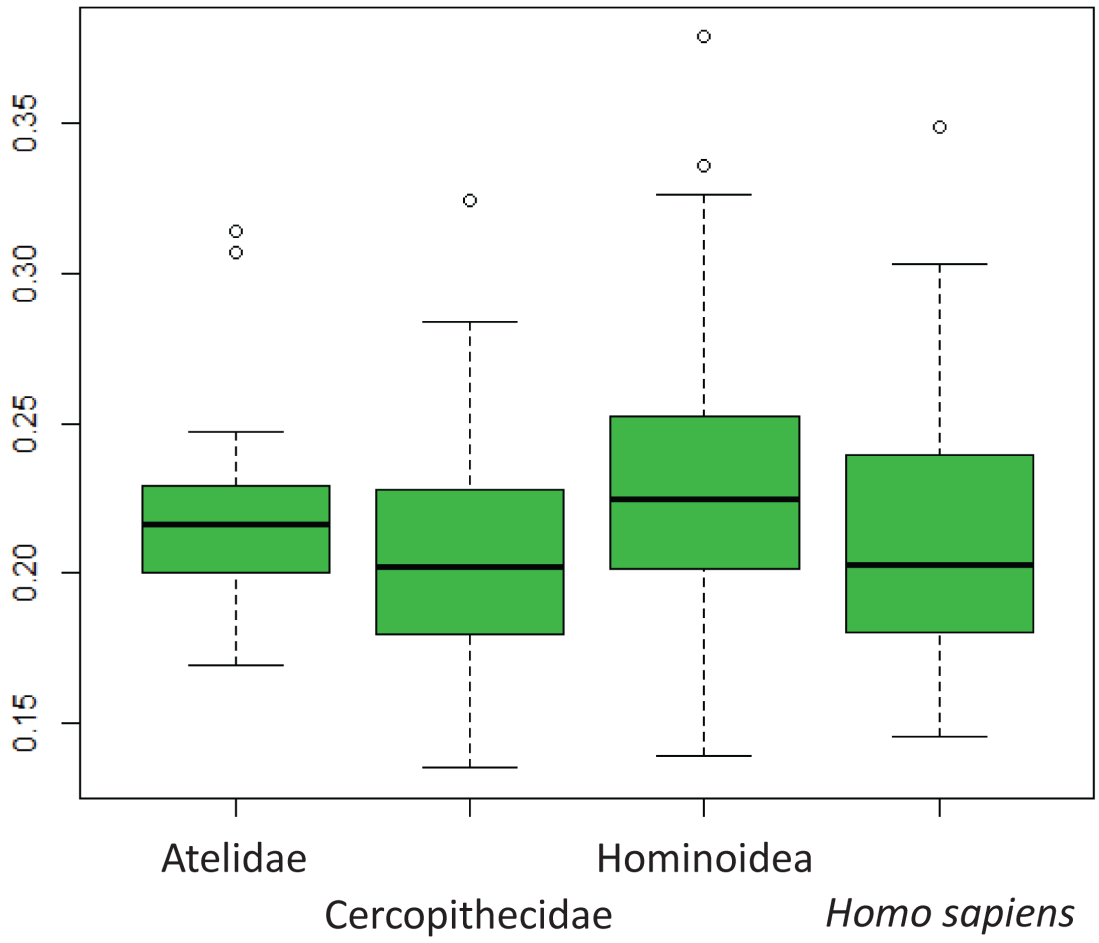

Figure 8: Boxplot comparing the pairwise Procrustes distances for *Ardipithecus ramidus* among taxonomic groups. Error bars indicate full range of the data. Points indicate outliers.

	Taxon	N
Platyrrhini		**21**
Atelidae	*Alouatta seniculus*	16
	Ateles spp.	5
Catarrhini		**103**
Cercopithecinae	*Macaca fascicularis*	14
	Macaca nemestrina	8
	Mandrillus spp.	13
	Papio spp.	18
Colobinae	*Theropithecus gelada*	4
	Colobus polykomos	6
	Nasalis larvatus	22
	Trachypithecus obscura	18
Hominoidea		**158**
Hylobatidae	*Hylobates spp.*	15
Hominidae	*Gorilla gorilla*	25
	Pan troglodytes	28
	Pongo pygmaeus	36
	Homo sapiens	54
Fossil Apes		**3**
	Proconsul heseloni KPS III RF3	1
	Oreopithecus bambolii BAC-83f	1
	Sivapithecus sp. GSP-19905	1
Fossil Hominins		**4**
	Ardipithecus ramidus ARA6-500-81	1
	Homo floresiensis LB1	2
	Homo habilis OH8	1

Table 1: Sample of cuboids analyzed for this project.

Landmark Number	Location	Equivalence to Harcourt-Smith (2002)
1	The medio-plantar corner of the distal articular facet for the 4th metatarsal	Landmark 3
2	The medio-dorsal corner of the distal articular facet for the 4th metatarsal	Landmark 1
3	The point at which the margin of the distal facets for the 4th and 5th metatarsals meet on the dorsal side	Landmark 4
4	The most lateral point of the distal facet for the 5th metatarsal	Landmark 6
5	The point at which the margin of the distal facets for the 4th and 5th metatarsals meet on the plantar side	Landmark 5
6	The midpoint of the peroneal groove on its medial side where the groove is most deep	New Landmark
7	The proximal margin of the peroneal groove on the lateral side	New Landmark

Table 2: List of landmarks taken on the cuboid and their equivalence to those taken by Harcourt-Smith (2002).

Locomotor Category	**Taxa**	**Reference**
Arboreal Quadruped	*Alouatta seniculus, Ateles spp., Colobus polykomos, Macaca fascicularis, Nasalis larvatus, Trachypithecus obscura*	Fleagle, 1999; Gebo, 1992; Mittermeier, 1978; Mittermeier and Fleagle, 1976; Rodman, 1979
Terrestrial Quadruped	*Macaca nemestrina, Mandrillus spp., Papio spp., Theropithecus gelada*	Fleagle, 1999; Rodman 1979
Brachiator	*Hylobates spp.*	Fleagle, 1999
Quadrupedal Climber	*Pongo pygmaeus*	Fleagle, 1999
Knuckle Walker	*Gorilla gorilla, Pan troglodytes*	Fleagle, 1999
Bipedal	*Homo sapiens*	Fleagle, 1999

Table 3: Taxa included in each locomotor category.

	Taxon	Groove Angle (°)
Atelidae		**9**
	Alouatta seniculus	10
	Ateles sp.	6
Cercopithecinae		**20**
	Macaca fascicularis	22
	Macaca nemestrina	18
	Mandrillus sp	22
	Papio sp.	21
	Theropithecus sp.	15
Colobinae		**22**
	Colobus polykomos	16
	Nasalis larvatus	23
	Trachypithecus obscura	22
Hominoidea		**19**
Hylobatidae	*Hylobates hoolock*	**30**
Great Apes		**14**
	Gorilla gorilla	13
	Pan troglodytes	17
	Pongo pygmaeus	14
Hominini	*Homo sapiens*	**23**
Fossil Apes		**14**
	Proconsul heseloni KPS III RF3	14
	Oreopithecus bambolii BAC-83f	8
	Sivapithecus sp. GSP-19905	21
Fossil Hominins		**25**
	Ardipithecus ramidus ARA6-500-81	24
	Homo floresiensis LB1	25
	Homo habilis OH8	25

Table 4: Mean groove angle values by taxon.

		Mean Difference	Standard Error	p-value	Lower 95% CI	Upper 95% CI
Atelidae	Cercopithecidae*	-11.85	1.68	<0.001	-16.47	-7.24
	*Hylobates**	-20.34	2.37	<0.001	-26.86	-13.83
	Great Apes*	-5.06	1.70	.026	-9.74	-0.39
	*Homo sapiens**	-13.38	1.80	<0.001	-18.333	-8.42
Cercopithecidae	Atelidae*	11.85	1.68	<0.001	7.24	16.47
	*Hylobates**	-8.49	1.94	<0.001	-13.82	-3.17
	Great Apes*	6.79	1.02	<0.001	4.00	9.58
	Homo sapiens	-1.53	1.18	.695	-4.76	1.71
Hylobates	Atelidae*	20.34	2.37	<0.001	13.83	26.86
	Cercopithecidae*	8.49	1.94	<0.001	3.17	13.82
	Great Apes*	15.28	1.96	<0.001	9.90	20.66
	*Homo sapiens**	6.97	2.05	.007	1.34	12.59
Great Apes	Atelidae*	5.06	1.70	.026	0.39	9.74
	Cercopithecidae*	-6.79	1.02	<0.001	-9.58	-4.00
	*Hylobates**	-15.28	1.96	<0.001	-20.66	-9.90
	*Homo sapiens**	-8.31	1.21	<0.001	-11.64	-4.99
Homo sapiens	Atelidae*	13.38	1.80	<0.001	8.42	18.33
	Cercopithecidae*	1.53	1.18	.695	-1.71	4.76
	Hylobates	-6.97	2.05	.007	-12.59	-1.34
	Great Apes*	8.31	1.12	<0.001	4.99	11.64

Table 5: Tukey HSD post-hoc test results comparing taxonomic groups. Stars indicate significance at the 0.05 level.

		Mean Difference	Standard Error	Significance	Lower 95% CI	Upper 95% CI
A Quad	T Quad	-2.89	1.34	.261	-6.74	0.96
	Brachiator	-11.64*	2.06	<0.001	-17.57	-5.72
	Suspensory	4.47*	1.48	.033	0.22	8.71
	KW	5.37*	1.68	.020	0.54	10.21
	Bipedal	1.021	1.61	.988	-3.62	5.66
T Quad	A Quad	2.89	1.34	.261	-0.96	6.74
	Brachiator	-8.75*	2.15	.001	-14.93	-2.57
	Suspensory	7.36*	1.60	<0.001	2.76	11.96
	KW	8.26*	1.79	<0.001	3.12	13.41
	Bipedal	3.91	1.73	.212	-1.05	8.87
Brachiator	A Quad	11.64*	2.06	.000	5.72	17.57
	T Quad	8.75*	2.15	.001	2.57	14.93
	Suspensory	16.11*	2.24	<0.001	9.67	22.55
	KW	17.02*	2.38	<0.001	10.18	23.86
	Bipedal	12.66*	2.33	<0.001	5.96	19.37
Suspensory	A Quad	-4.47*	1.48	.033	-8.71	-0.22
	T Quad	-7.36*	1.60	<0.001	-11.96	-2.76
	Brachiator	-16.11*	2.24	<0.001	-22.55	-9.67
	KW	0.91	1.90	.997	-4.55	6.36
	Bipedal	-3.45	1.84	.419	-8.72	1.83
KW	A Quad	-5.37*	1.68	.020	-10.21	-0.54
	T Quad	-8.26*	1.79	<0.001	-13.41	-3.12
	Brachiator	-17.02*	2.38	<0.001	-23.86	-10.18
	Suspensory	-.91	1.90	.997	-6.36	4.55
	Bipedal	-4.35	2.00	.256	-10.11	1.41
Bipedal	A Quad	-1.02	1.61	.988	-5.66	3.62
	T Quad	-3.91	1.73	.212	-8.87	1.05
	Brachiator	-12.66*	2.33	<0.001	-19.37	-5.96
	Suspensory	3.45	1.84	.419	-1.83	8.72
	KW	4.35	2.00	.256	-1.41	10.11

Table 6: Tukey HSD post-hoc test results comparing locomotor groups. Stars indicate significance at the 0.05 level. Abbreviations: A Quad = Arboreal Quadruped, T Quad = Terrestrial Quadruped, KW = Knuckle Walker.

Dependent Variable	Type III Sum of Squares	Degrees of Freedom	Mean Square	F Statistic	P-value
PC 1	0.965	7	0.138	49.193	<.001
PC 2	0.594	7	0.085	31.994	<.001
PC 3	0.352	7	0.050	30.844	<.001
PC 4	0.170	7	0.024	13.747	<.001
PC 5	0.211	7	0.030	28.189	<.001
PC 6	0.033	7	0.005	4.113	<.001
PC 7	0.057	7	0.008	8.503	<.001

Table 7: Results of the MANOVA comparing taxa on PCs 1 – 7.